6

Neutron Induced Structural and Electrical Response of $BaSrTiO_3$ Interdigitated Capacitor

6.1 INTRODUCTION

Perovskite oxide materials have shown potential for obtaining voltage tunable materials for development of microwave-tunable devices over broad frequency [Subramanyam *et al*, 2013]. Voltage tunable components with multifunctional oxides can provide new capabilities along with the possibility of simultaneous receive and transmit. In addition, perovskite oxide materials are known as radiation hard materials with better dielectric properties [Scott *et al*, 1991; Morre *et al,* 1991]. We have investigated gamma radiation induced structural and electrical changes in BST thin film in previous chapter.

The neutrons are produced in nuclear reactor as well as in space orbits, give exposure to the material which can affect sensor and control circuits. Neutrons are highly penetrating and capable of bringing about irreversible microstructural changes in nuclear environments where exposure to energetic neutrons can dramatically alter the performance of a material [Kinchin *et al*, 1955]. Next generation communication devices with applications of wireless technology are emerging requirements with use of suitable neutron resistant material. Fast neutron undergo scattering collisions with atomic nuclei, give rise to damage accumulates, in turn produces localized displacement cascades and subsequent interaction of mobile and immobile defect species i.e. vacancies, self-interstitial atoms, and point defect clusters [Chroneos *et al,* 2012]. Interest in radiation effects on BST thin films also important for memory and tunable applications in nuclear power and satellite technology where the total device lifetime determined by radiation damage [Rebeiz and Muldavin, 2001]. The physical interpretation of a decrease in dielectric characteristics is that local wells in the free energy regime associated with domain wall configuration become narrower with neutron fluence; might be due to an increase in the density of pinning sites [Graham *et al*, 2013]. Moreover it is known that microstructural features act as sinks for radiation induced mobile defect clusters and point defects [Golubov *et al,* 2012]. The leakage current density was found to increase with increasing radiation dose and linked with charge trapping along with the generation of defect clusters that causes of leakage current conduction in oxides. The foremost step for the occurrence of leakage current is the generation of defect clusters, prior to the total destruction of the capacitor structure. The radiation response of varactor devices for use in radiation environment is thus a topic of significant importance and several studies suggest that radiation induced trapping in the high-k perovskite is an important problem. Therefore, it is desired to understand their radiation response before these high-k dielectrics can be used for nuclear and space applications. The perovskite structures, usually consisting of two or more cations with different chemical nature and precise influence of irradiation are difficult to invstigate on the macroscopic properties due to their complex structure [Zinkle *et al*, 2012]. Several studies have been carried out on $PbZrTiO_3$ and $PbLaZrTiO_3$ which demonstrated that neutron irradiation leads to considerable changes in dielectric behavior [Moore *et* al, 1991; Kulikov *et al,* 2012]. Originally, Silicon-on-Sapphire (SOS) was used for the radiation-hard applications. However, there is only one report on neutron irradiation stability of BST thin film [Glinsek *et al*, 2015], whereas no report on BST based varactor. Hence it is worth to investigate neutron irradiation effects on the electrical properties of BST varactors.

We report in this chapter, neutron irradiation resistance of the barium strontium titanate (BST) thin film based varactor under different neutron fluences. BST thin films were deposited on sapphire substrate by RF magnetron sputtering and IDC electrodes were patterned with photolithography technique. Reliability of neutron irradiated BST varactors were studied along with investigation of structural and morphological characterizations. C-V and leakage current characteristics were measured at several neutron fluences. A small change in capacitance is observed at different fluences. The changes are attributed to the radiation-induced defect dipoles and other charged defects. We supplemented this macroscopic *C-V* behavior of BST varactor with investigation through X-ray diffraction and atomic force microscopy for their structural and morphological changes, respectively. This study shows that BST varactor can be used in neutron environment due to its high tolerance.

6.2 EXPERIMENTAL DETAILS

6.2.1 Sample Preparation

$Ba_{0.5}Sr_{0.5}TiO_3$ films were deposited on sapphire substrate by RF magnetron sputtering. The polished crystalline r-plane sapphire wafers were cleaned by standard semiconductor cleaning process using Trichloroethylene, Methanol and Acetone. 200 nm thick BST films were deposited with rate of 0.2 µm/hr. Subsequently, deposited films were annealed at temperature 800°C in oxygen ambient which completes the oxygen deficiencies and leads to phase formation. The IDC structure has wide surface area than vertical MIM structure and preferred to study the electrical response at high radiation exposure. The IDCs were patterned using photolithography and lift-off techniques. Total 10 fingers of Au/Ti were patterned with finger dimension of 5 µm width, 390 µm length and spacing 3 µm as shown in Figure 6.1. The phase composition and the orientation of the BST films were investigated using XRD and surface morphology were analysed using AFM.

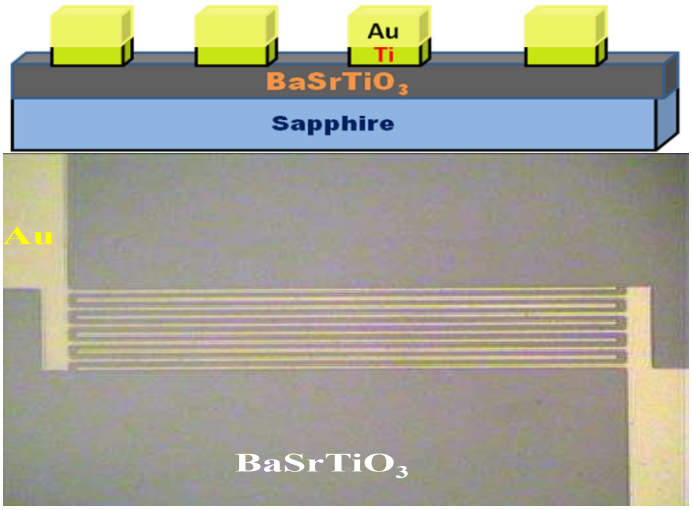

Figure 6.1: Schematic cross-section view and optical image of gold plated IDC structured Device.

6.2.2 Neutron Irradiation

The fabricated IDC devices were irradiated for different neutron fluences using ^{252}Cf radioactive source. The ^{252}Cf spontaneous neutron source is relatively clean source, which has relatively well measured neutron spectra. Average neutron energy in the californium spectrum is 2.1 MeV. The ^{252}Cf isotope is an intense neutron emitter. It decays by alpha emission and spontaneous fission with half life of 2.645 y. The ^{252}Cf neutron source is housed in multi cylindrical tube to appropriately shield the alpha particles and fission fragments. The samples were kept in neutron irradiation facility to irradiate up to fluence of $7.5x10^{11}$ n/cm^2.

6.3 STRUCTURAL AND SURFACE MORPHOLOGICAL CHARACTERIZATIONS

The structural analysis by X-ray diffraction revealed significant modifications in diffraction peaks. The structural modification strongly depends on irradiated ions and their fluences. The XRD 2θ-ω scans were recorded on all the samples and shown in Figure 6.2. It reveals perovskite structure of BST film with the diffraction peaks of (110) at $2\theta=31.85^0$ and (111) at $2\theta=39.30^0$. A slight change in peak position and full width half maximum (FWHM) are observed with increasing neutron fluences. The radiation-induced degradation in ferroelectric properties is generally affected by defects resulted from two main factors which are the atom-displacement effects and ionizing effects. Neutron induced defects such as vacancies, interstitials and displacements increase the FWHM of diffraction peak and decreased the crystallinity of BST thin films.

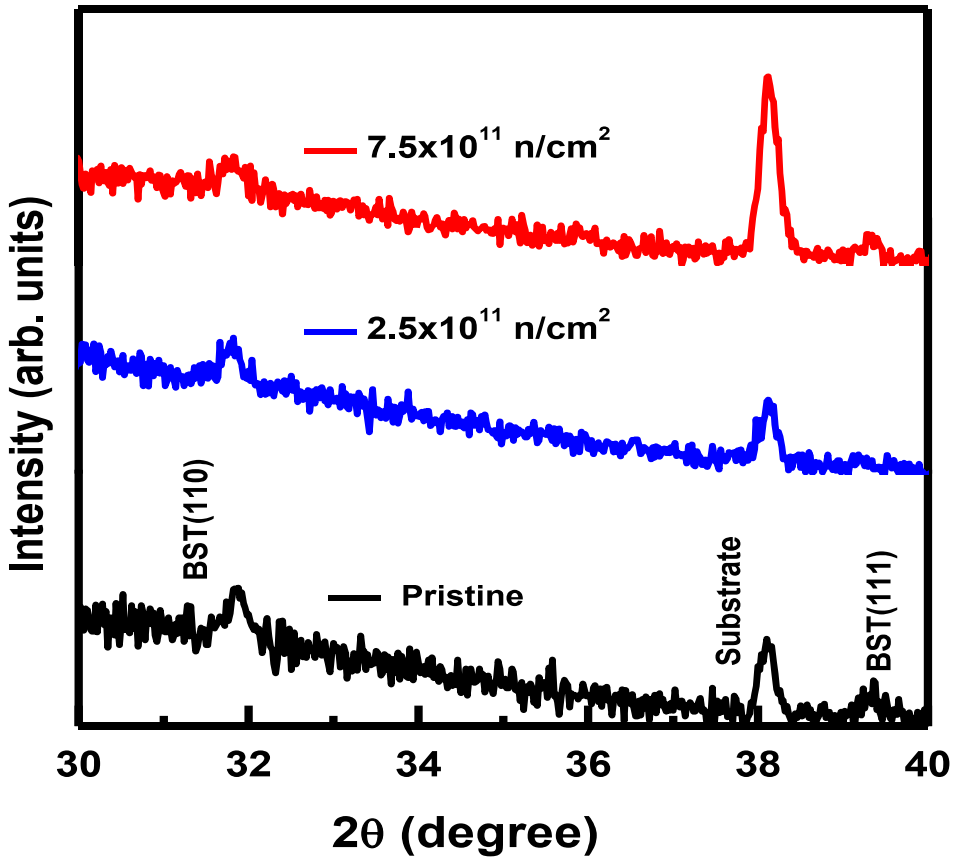

Figure 6.2: XRD 2θ-ω scan of BST thin film before and after neutron irradiation

Neutron irradiation also affects the internal stress of thin film and shift XRD peak towards to lower angles. Fig. 6.2 shows the variations of intensities of XRD patterns at (110) plane of BST thin film sample as increasing neutron irradiation dose. The increased FWHM, represents the gradual decrease in crystallinity with increasing irradiation fluence. Figure 6.3 shows AFM image of BST thin films and it can be observed that roughness of film surface increases with neutron fluences. The root mean square (RMS) roughness of pristine sample is 4.6 nm and highest RMS value of 6.5 nm for $7.5x10^{11}$ n/cm^2 neutron irradiated sample.

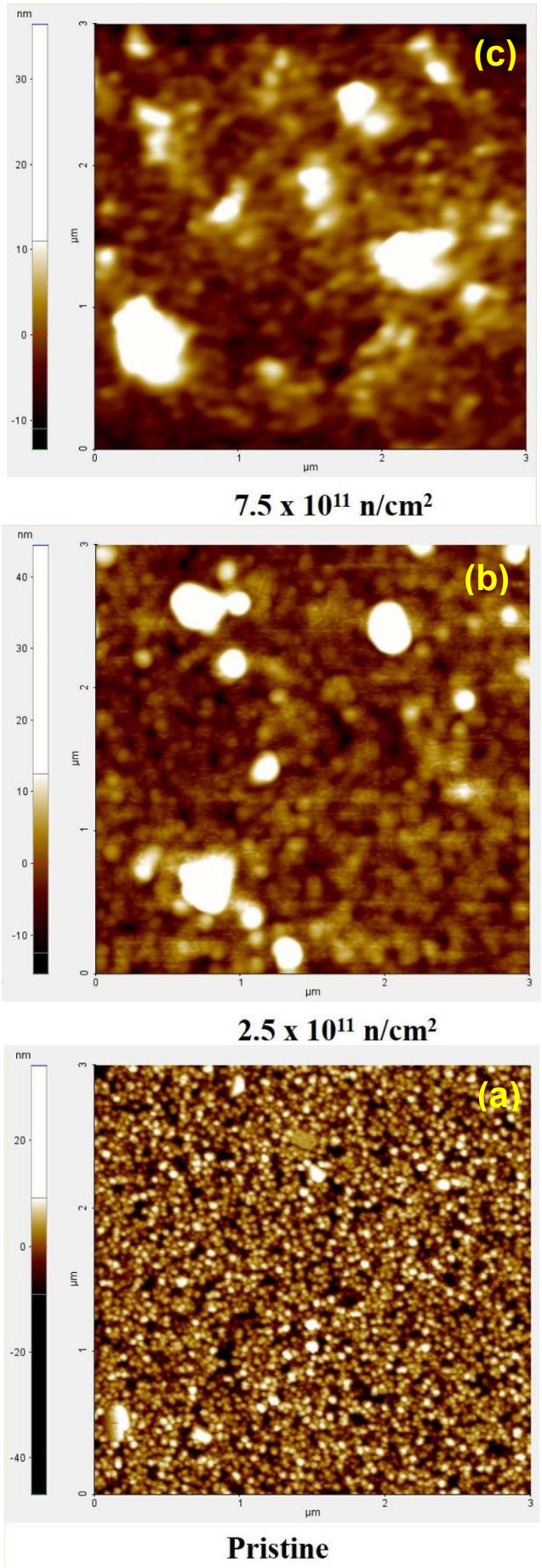

Figure 6.3: AFM images (3 x 3 μm^2) at different neutron fluencies a) Pristine b) 2.5x10^{11} n/cm^2 c) 7.5x10^{11} n/cm^2

6.4 ELECTRICAL CHARACTERIZATION

Electrical characterizations (*C-V* and *I-V*) were carried out using Semiconductor Characterization System (Keithley SCS 4200) before and after neutron irradiation for different fluence with a constant time difference after each exposure to account for prolonged generation of interface states. The *C–V* curves were measured at different frequencies from 200 kHz to 500 kHz. DC bias swept has been performed with signal amplitude of 60 mV from -30 V to +30 V at a rate of 0.25 V/s.

6.4.1 Capacitance – Voltage (C-V) Measurements

Figure 6.4 shows the evolution of the capacitance versus applied bias (C-V) curves of pristine IDC device and these curves present the classical "bell" shaped loop as expected and attributed by changing the direction of polar molecule depending upon the applied electric field. The capacitance of the device was investigated as a function of neutron fluences at two different frequencies of 200 kHz and 500 kHz as shown in Figure 6.5. A slight reduction of the maximum capacitance is observed with increasing neutron fluences up to 2.5×10^{11} n/cm^2 and the capacitance of the IDC structured device is slightly lower than that of the pristine device for both 200 kHz and 500 kHz frequency.

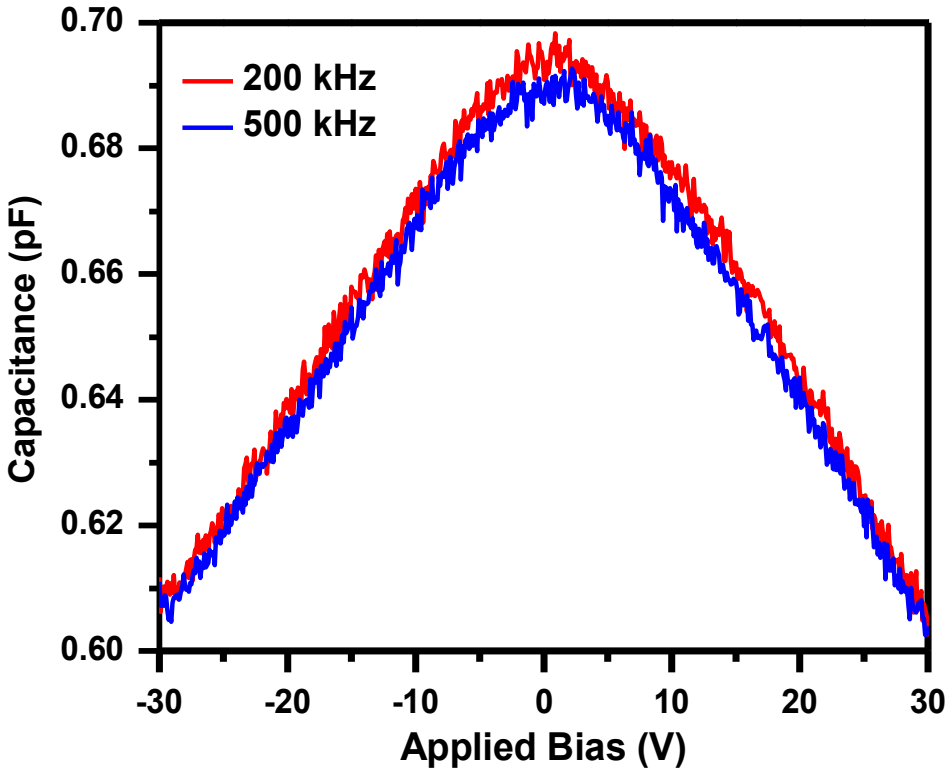

Figure 6.4: Bell shape C-V behavior of pristine BST varactor at 200 kHz and 500 kHz frequency

From Figure 6.5, it was also observed that the maximum capacitance value of the device is gradually increased after 2.5×10^{11} n/cm^2 fluence and reached closer to the value of pristine device for the neutron fluence of 5.0×10^{11} n/cm^2 and 7.5×10^{11}n/cm^2. Conclusively the maximum capacitance of IDC device was found to decrease initially with the neutron fluence and the capacitance value rises for neutron fluence of 5.0×10^{11} n/cm^2 and 7.5×10^{11} n/cm^2 where the capacitance is close to the pristine device.

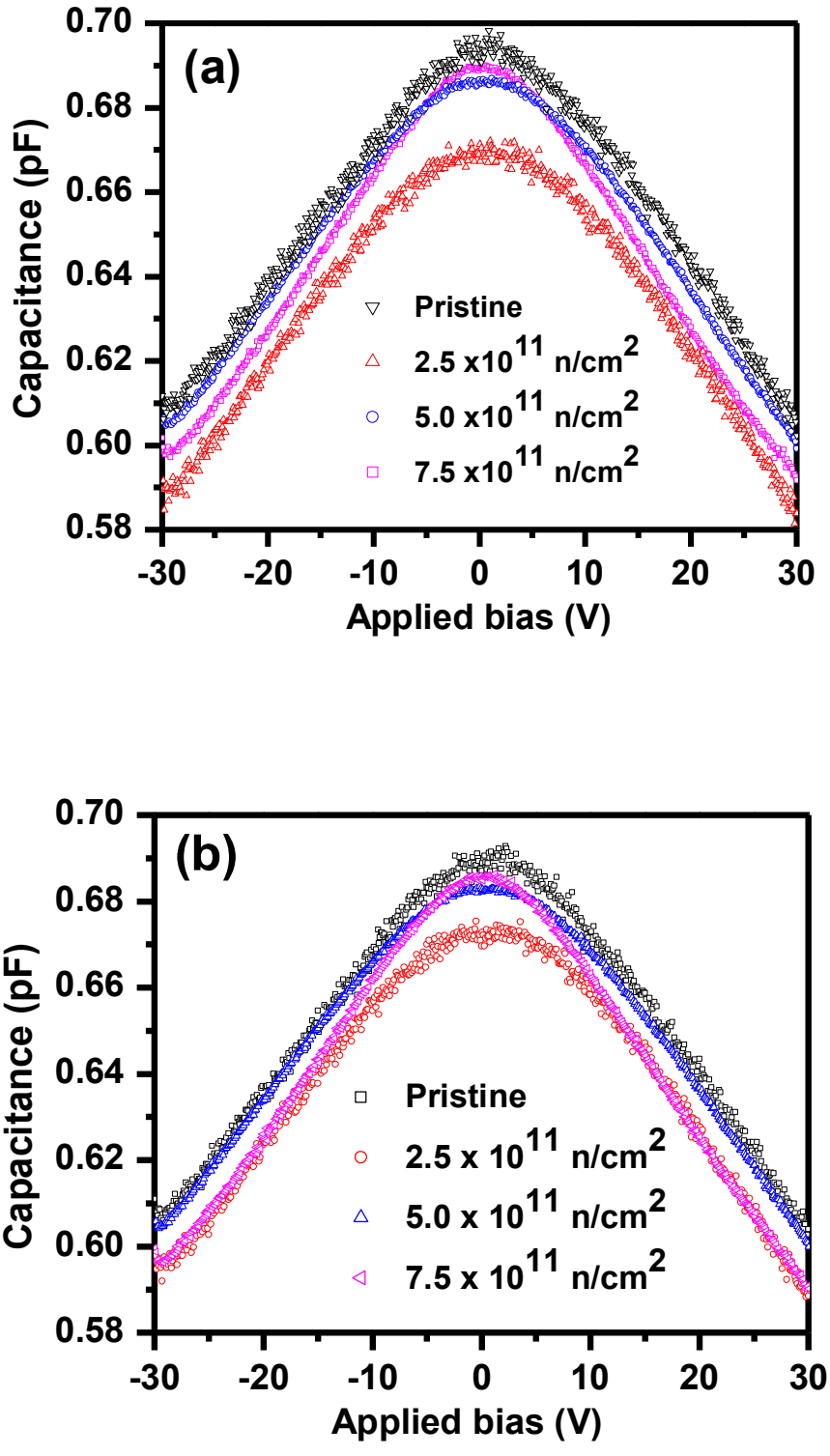

Figure 6.5: The capacitance as a function of the neutron fluencies at (a) 200 kHz and (b) 500 kHz frequency

Radiation induced changes are expected while irradiating the device by neutrons and the radiation damage caused exclusively due to point defects. In neutron irradiations the densities of the primary defects are very large compared to the densities that occur in gamma irradiation at the end of a Primary Knock on Atom (PKA) cascade, hence neutrons produce far more di-vacancies and higher-order vacancies than gammas [Moll *et al,* 1997]. High energy neutron irradiation can displace large number of atoms from their own site to the other sites,

which lead to produce some defects such as interstitials, impurities, and vacancies. These defects can be easily accumulated along the domain walls and grain boundaries, which could lead to the pinning of the domain walls. On the other hand, large amounts of the electron-hole pairs could also be generated by ionizing effects and might trapped by radiation-induced defects. These trapped charges can produce a local field to the opposite direction of the external field, which results in the degradation of polarization. Neutron irradiation give rise to produce mostly oxygen vacancies defects in ABO_3 varactor [Bittner *et al*, 2004; Ang *et al*, 2000]. Oxygen vacancies leads to capacitive change in BST film due to the vacancy forced distortion of the B-site atoms in 'c' direction. An accumulation of these charged oxygen vacancies traps polarization domains hence reduces maximum capacitance for $2.5x10^{11}$ n/cm^2 fluence. In addition mobile charge carriers are generated, which are trapped by defects, such as oxygen vacancies, grain boundaries, or interfaces and build up an internal bias field or increase the space charge polarization as well as the conductivity. The change in the electrical properties as shown in Figure 6.5 of the device can be attributed to the generation of the V_2O center [Huhtinen, 2002], rightfully be considered for the IDC structured BST film for an understanding of macroscopic damage effects. Decrease of the capacitance may also be explained by a combination of "dilution" and intrinsic size effect due to the low permittivity grain boundaries [Frey *et al,* 1996]. It has been believed that grain boundary layer is characterized by low polarization and low capacitance layer due to its highly atomic disordered region, even amorphous, or with relaxed tetragonality. Hence the decrease of crystallinity of the BST thin film is related to the increase of defect density of the sample, may causes the decrease of permanent dipole moment [Hoshina *et al,* 2008]. It is also suggested that Ba atom and oxygen vacancy site likely play a role in domain wall pinning as similarly reported by Henriques *et al* in PZT ferroelectric materials due to neutron irradiation [Henriques *et al*, 2014]. Neutron-induced defects in the perovskite lattice may result in charge trapping which can induce domain wall pinning and thus influence the dielectric properties of the film [Moore *et al*, 1991]. Defect complexes in perovskite films such as di-vacancies or impurity vacancy associates carry a dipole moment [Cockayne *et al*, 2004]. The neutron irradiation leads to the qualitatively similar variation of switching current shape as electron irradiation. The observed effects have been attributed to the acceleration of the bulk screening induced by irradiation [Kuznetsov *et al*, 2006]. The observed behavior could be explained in combination of crystallinity, grain size effect, oxygen defects and mobile carriers generated during neutron irradiation.

With higher neutron fluence, both positively and negatively poled features can be created, trapped charge buildup, establishing a local electrical field, which switches the underlying polarization [Li *et al*, 2006]. The mechanism of polarization process plays important role to increase the capacitance of the device after certain fluence [Mane *et al*, 2011]. A gradual formation of space charge polarization or mobile charge carriers where the electron exchange interaction may result in local displacement of the electron in the electric field direction and increases the capacitance at higher radiation exposure [Li and Kraner, 1992; Tataroglu *et al*, 2007; Sinha *et al*, 2001; Al-karmi *et al*, 2006].

6.4.2 Leakage Current Study

Conduction mechanisms in (Ba,Sr)TiO3 and Pb(Zr,Ti)O3 thin films have previously been studied and observed that the leakage current is controlled by the bulk of the film and the interfaces with the electrodes where one of them is highly dominant in most of the cases. The applied bias dependence of the leakage currents was measured on BST varactor to investigate the irradiation effects, before and after irradiation at different neutron fluence. Total five varactors were tested and a good reproducibility was obtained. I-V characteristics of the BST varactor is shown in Figure 6.6 at different neutron fluence and observed that leakage current increases as a function of neutron fluences [Li and Kraner, 1992; Liu *et al*, 2012]. Neutron irradiation, result in the high density of acceptor like electron traps, donor like traps, preexisting traps and generated traps in high-k dielectrics. Similarly gamma irradiations were considered for changes in current voltage characteristics [Miao *et al*, 2009]. The dominant intrinsic defects in high-k materials are oxygen related defect mechanism as investigated by experimental observations using point defect modeling [McIntyre, 2007]. The oxygen related

defects are mainly present in the form of oxygen interstitials, vacancies, oxygen deficiency and charged oxygen vacancies. High leakage current due to neutron irradiation can also be explained by increasing the defect density which provides conduction path between electrodes by charge hopping between proximate traps. The oxygen vacancies at the surface pins the fermi level of the BST and top metal (Au) electrode close to the conduction band minimum, in turn lowering schottky barrier height [Schafranek *et al*, 2010]. Dielectric loss is also associated with increase in leakage current where it is coupled with the resistive losses [Cole *et al*, 2003]. The results are in correlation with the effects of point defects, generated by the neutron and gamma radiation to our previous work on gamma irradiation induced response on tunable capacitor. Therefore C-V measurements in BST varactor is influenced by mobile charge carriers, generated by neutron irradiation which might have contributed into drifting inside as well as along the grain boundaries in response to the bias voltage [Schroder, 1998].

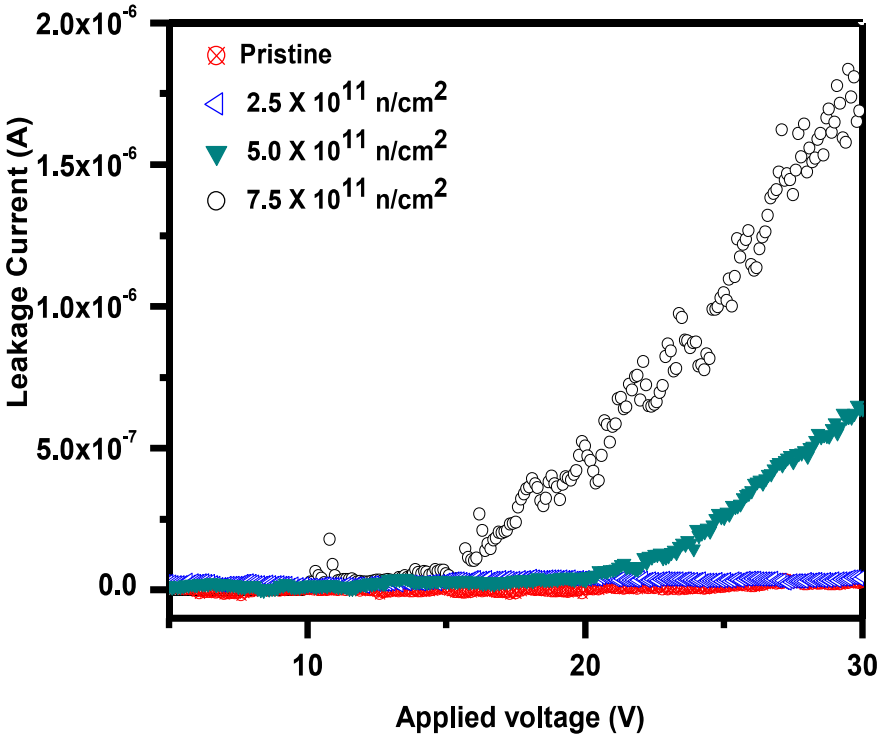

Figure 6.6: Leakage current characteristics of IDC capacitor ation as function neutron fluences.

6.5 CONCLUSIONS

The neutron induced effects on BST based tunable varactors have been investigated. The changes in the electrical properties by irradiation to the device could be attributed by induces defects, displacement damage, causes to structural changes which have been revealed from XRD. The observed decrease in capacitance for lower neutron fluence and a significant rise in capacitance value towards pristine device at higher neutron fluences of $5x10^{11}$ n/cm^2 and $7.5x10^{11}$ n/cm^2, indicates the presence of the different type of defects in the BST film. The increased number of defects and grain boundary due to neutron irradiation serves as current path and confirmed by increasing leakage current characteristics. Also the presence of space charge polarization caused due to structural changes may be associated to the increase in capacitance value after certain neutron fluence. AFM results confirm increasing roughness of the surface and degraded the surface quality with increasing neutron irradiation.